

Complete phenomenological gravitational waveforms from spinning coalescing binaries

R. Sturani^(1,2), S. Fischetti⁽³⁾, L. Cadonati⁽³⁾, G. M. Guidi^(1,2), J. Healy⁽⁴⁾, D. Shoemaker⁽⁴⁾, A. Viceré^(1,2)

(1) *Dipartimento di Matematica, Fisica e Informatica,*

Università degli Studi di Urbino 'Carlo Bo', I-61029 Urbino, Italy

(2) *INFN Sezione di Firenze, I-50019 Sesto Fiorentino, Italy*

(3) *Physics Department, University of Massachusetts, Amherst MA 01003, USA*

(4) *Center for Relativistic Astrophysics, Georgia Tech, Atlanta, GA 30332, USA**

The quest for gravitational waves from coalescing binaries is customarily performed by the LIGO-Virgo collaboration via matched filtering, which requires a detailed knowledge of the signal. Complete analytical coalescence waveforms are currently available only for the non-precessing binary systems. In this paper we introduce complete phenomenological waveforms for the dominant quadrupolar mode of generically spinning systems. These waveforms are constructed by bridging the gap between the analytically known inspiral phase, described by spin Taylor (T4) approximants in the restricted waveform approximation, and the ring-down phase through a phenomenological intermediate phase, calibrated by comparison with specific, numerically generated waveforms, describing equal mass systems with dimension-less spin magnitudes equal to 0.6. The overlap integral between numerical and phenomenological waveforms ranges between 0.95 and 0.99.

I. INTRODUCTION

The Laser Interferometer Gravitational-wave Observatory (LIGO) and Virgo constitute a network of kilometer-scale interferometers for the detection of gravitational waves. The initial detector configuration has successfully acquired data at design sensitivity; substantial upgrades over the next few years, to Advanced LIGO and Advanced Virgo, are expected to yield the detection of gravitational waves from the coalescence of compact binary systems of neutron stars or black holes.

The coalescence of binary systems is usually described in terms of three distinct phases: the inspiral, the merger and the ring-down. The inspiral phase allows for an accurate analytical description via the so-called Post-Newtonian (PN) expansion, see for instance [1] for a review. The ring-down also admits a perturbative analytical model, as it describes the damped oscillations of the single object resulting from the binary coalescence, as a superposition of black-hole quasi normal modes [2]. The merger phase is however fully non-perturbative and for generic systems it has not been described analytically but rather by numerical simulations. During the last five years numerical relativity has made tremendous progress in describing the full coalescence of a binary system beginning with [3–5] and more recently [6–12], see [13–15] for reviews and it can now produce waveforms for generic spin orientations, with moderate spin magnitude ($\lesssim 0.9$) and mass ratios ($\lesssim 10 : 1$).

Matched filtering is typically used in LIGO-Virgo data analysis in order to uncover weak signals buried into noise [16]. This technique requires a large number (tens of thousands) of templates to be checked against real data. Due to the computational cost of numerical simulations, this is only possible with an analytical knowledge of the templates. Analytical methods are currently available to reproduce the complete waveform emitted by non-precessing coalescing binaries. This has been achieved in the Effective One Body (EOB) construction [17–19] for non-spinning systems, and in the EOB-spin waveforms [20], an extension of the EOB method to the case of binaries with non-vanishing spins aligned with the orbital angular momentum. Both spinning and non spinning EOB require a comparison with numerically generated waveforms in order to calibrate some free parameters of the model. Another method for generating analytical waveforms for spinning non-precessing binaries is by joining PN-generated inspiral and numerical waveforms [10, 21] to construct phenomenological waveforms.

In this paper we present a new family of analytical waveforms from the coalescence of generic spinning binaries.

The waveforms are obtained by interpolating between the perturbative PN inspiral description and the ring-down, both admitting physically motivated analytic models, with a phenomenological phase over the merger portion of the signal. Since in the matched-filtering search an accurate determination of the gravitational phase of the signal is crucial, more important than an accurate amplitude determination, we focus on the phenomenological parametrization of the gravitational wave phase, and give lower priority to the amplitude.

Spinning waveforms depend on several parameters (masses, spin components of the binary constituents, angles defining

*Electronic address: riccardo.sturani@uniurb.it

the orientation of the source with respect to the observer). For this reason it is not practical to use these waveforms to build template banks, but we envision their usefulness as injection waveforms in testing existing LIGO-Virgo data analysis pipelines, which are currently based on non-spinning templates.

The paper is organized as follows. In sec. II the method for the analytical waveform construction and the numerical simulations are illustrated. In sec. III the results are presented, in the form of comparison between analytically and numerically generated waveforms. We restricted the analysis to the main quadrupolar mode ($m = 2$), but this setup can be extended to include other modes. In sec. IV the conclusions that can be drawn from the present work are reported.

II. THE METHOD

The goal of the present work is to produce the complete analytical waveforms generated by the coalescence of spinning binary systems. The numerical waveforms used to construct and calibrate our analytical model all describe equal mass binary systems ($m_1 = m_2$), with spin magnitudes $|\mathbf{S}_1| = |\mathbf{S}_2| = 0.6 m_1^2$ and \mathbf{S}_2 orthogonal to the initial orbital angular momentum (where $\mathbf{S}_{1,2}$ denote the binary constituent spin vectors and we posit $G_N = c = 1$).

The description of the dynamics adopted here models the inspiral phase via the standard TaylorT4 PN formulas, see [22] for definition and comparison of different PN approximants in the spin-less case. In the non-spinning case the waveform is fully parametrized by amplitude and the orbital phase, but in the spinning case the effect of the precession of the orbital plane should also be accounted for, see [23] spin and angular momentum evolution equations. It is convenient to define an orbital phase $\phi = \int \omega_{orb} dt$ whose evolution is given by

$$\frac{d\phi}{dt} = \frac{v^3}{M}, \quad \frac{dv}{dt} = -\frac{F(v)}{dE/dv}, \quad (1)$$

where $M \equiv m_1 + m_2$ is the total mass of the binary system, $F(v)$ and $E(v)$ are respectively the flux emitted and the energy of a circular orbit with angular frequency $\omega_{orb} = v^3/M$. The main gravitational wave frequency f_{GW} is related to ω_{orb} via $f_{GW} = \omega_{orb}/\pi$.

In order to determine the actual waveform also the spins and the orbital angular momentum have to be dynamically evolved, see e.g. [24]. In particular by parametrizing the orbital angular momentum unit vector $\hat{\mathbf{L}}$ as $\hat{\mathbf{L}} = (\sin \iota \cos \alpha, \sin \iota \sin \alpha, \cos \iota)$ it is convenient to introduce the carrier phase Ψ given by

$$\frac{d\Psi}{dt} = \omega_{orb} - \cos \iota \frac{d\alpha}{dt}. \quad (2)$$

Numerically generated waveforms are usually decomposed in spherical harmonics, in particular the five quadrupolar modes ($l = 2$) are the only non-vanishing at the lowest order in v , and the $l = 2, m = \pm 2$ mode are the dominant ones. The actual shape of the $l = 2, m = 2$ mode, the only one which will be used here for comparison with numerical relativity results, is given by the following [24]

$$h_{2,2}^{(insp)} = -2 \frac{\nu M v^2}{d} \sqrt{\frac{16\pi}{5}} [\cos^4(\iota/2) \cos(2(\Psi + \alpha)) + \sin^4(\iota/2) \cos(2(\Psi - \alpha)) + O(v)], \quad (3)$$

where $\nu \equiv m_1 m_2 / M^2$ is the symmetric mass ratio, d the source-observer distance and this formula refers to the inspiral waveform only.

The functions $F(v)$ and $E(v)$, necessary to determine the orbital phase, are known up to 3.5PN order as far as orbital effects are concerned, and up to 2.5PN and 2PN level for respectively $\mathbf{S}_{1,2}\mathbf{L}$ and $\mathbf{S}_1\mathbf{S}_2, \mathbf{S}_1\mathbf{S}_1, \mathbf{S}_2\mathbf{S}_2$ interactions.

According to studies in the non-spinning case [18, 25, 26], the TaylorT4 appears to be a very good approximant up to a frequency $\bar{\omega} = \pi \bar{f}_{GW} \simeq 0.1/M$ for the equal mass case, even though its faithfulness seems to worsen for different mass-ratios.

The PN evolution is halted when ω_{orb} reaches the value ω_m that is determined by comparison with numerical waveforms. For $\omega_{orb} > \omega_m$ (ω_{orb} is monotonic here) the angular frequency is evolved according to

$$\omega_{orb}(t) = \frac{\omega_1}{1 - t/T_A} + \omega_0, \quad \omega_m < \omega_{orb} \text{ and } t < t_{rac}, \quad (4)$$

where the three unknown parameters $\omega_{0,1}$ and T_A are fixed by requiring that $\omega_{orb}, \dot{\omega}_{orb}$ and $\ddot{\omega}_{orb}$ be continuous at the matching point defined by ω_m , and t_{rac} will be defined shortly. In this phenomenological phase the amplitude of the waveform is evolved according to the lowest order formula eq.(3), with ι and α frozen to their values at the instant

of time when $\omega_{orb} = \omega_m$ (and keeping as usual $v = (M\omega_{orb})^{1/3}$) [34].

After this phenomenological phase, in order to smoothen the evolution of ω_{orb} , which should settle at the ring-down value ω_{rd} , it turned out useful to join the time evolution of eq.(4) with a smoothing function

$$\omega_{orb}(t) = \omega_{rd} - \left(1 - \frac{t}{T_A}\right)^2 \omega_2 \quad t_{rac} < t \text{ and } \omega_{orb} < \omega_{mrd} \equiv 0.8\omega_{rd} \quad (5)$$

where t_{rac}, ω_2 are fixed by requiring continuity of ω_{orb} and $\dot{\omega}_{orb}$. For $\omega_{orb} > \omega_{mrd} = 0.8\omega_{rd}$ the waveform is described by the damped exponential

$$h_{2,2}^{(rd)} = e^{-t/\tau} [A \cos(\omega_{rd}t) + B \sin(\omega_{rd}t)] , \quad (6)$$

where A and B are constant to be determined requiring the continuity of $h_{2,2}$. For each multipolar mode defined by a pair l, m there is an infinity of overtones with increasing damping factor, but for our practical purposes retaining only the first overtone is enough.

Note that the degree of continuity of the waveform across the phenomenological -ring-down phase transition is not affected by changing the value of ω_{mrd} , but only by the number of overtones admitted to describe the ring-down phase in eq. (6), as it happens in the EOBNR construction [27].

The values of the ring-down frequencies and damping factors of the three lowest overtones of the $l \leq 4$ modes can be read from [28] as a function of the mass and spin of the final object created by the merger of the binary system. The final mass is determined by the algebraic sum of the constituents' masses and the negative binding energy once ω_m is reached, and the final spin according to the phenomenological formula given in [29].

The damped exponential is attached when ω_{orb} reaches 80% of the ω_{rd} value as it turned out that this specific value allowed the best overlap between analytical and numerical waveform, irrespectively of the initial spins.

The analytical waveforms just described has been quantitatively confronted with the numerically generated ones by computing the overlap integral

$$I_{h_1, h_2} \equiv \int h_1(f) h_2^*(f) df , \quad (7)$$

maximized over initial phase and time of arrival. The angular frequency ω_m has been determined by a first set of numerically produced short waveforms (4-6 cycles long) by picking the value which allowed a maximum overlap integral with the phenomenological waveform, with a determination precision of $\pm 10^{-4}/M$.

The numerical waveforms used in the present work have been generated with **MayaKranc**. The grid structure for each run consisted of 10 levels of refinement provided by **CARPET** [30], a mesh refinement package for **CACTUS** [31]. Sixth-order spatial finite differencing was used with the BSSN equations implemented with **Kranc** [32]. The outer boundaries are located at $317M$ and the finest resolution is $M/77$. Waveforms were extracted at $75M$. A few waveforms were generated at resolutions of $\{M/64, M/77, M/90\}$, and convergence consistent with our fourth order code is found. The short (long) runs showed a phase error on the order of $5 \cdot 10^{-3}$ ($5 \cdot 10^{-2}$) radians and an amplitude error of $\approx 2\%$ ($\approx 5\%$). We expect similar accuracy in all runs performed.

The numerical waveforms describe the $l = 2, m = 2$ mode and consist of two sets, both with equal mass and spin magnitudes $|\mathbf{S}_1| = |\mathbf{S}_2| = 0.6m_1^2$. The first set consisted in 24 few-cycle-long waveforms, representing mostly the merger and ring-down phases of a coalescence. They have been used to fix the values of ω_m for the corresponding values of initial spins. One of the binary constituent had initial spin $\mathbf{S}_2/m_1^2 = (-0.6, 0, 0)$ in the reference frame in which the initial $\hat{\mathbf{L}} = (0, 0, 1)$. The different values of the first dimension-less spin have been obtained by rotating the $(0, 0, 0.6)$ vector by 15 degrees in the x-z plane. Once determined the values of ω_m for each waveform, the value of the matching frequency ω_m for generic spins has been determined by assuming an analytical dependence of ω_m on $\mathbf{S}_{1,2}$, according to

$$M\omega_m = a_0 + a_1(S_{1z} + S_{2z}) + a_2\delta(S_{1z} - S_{2z}) + a_3(S_1 S_2)_\perp + a_4(S_{1\perp}^2 + S_{2\perp}^2) + a_5\delta(S_{1\perp}^2 - S_{2\perp}^2) + a_6(S_{1z}^2 + S_{2z}^2) + a_7(S_{1z} S_{2z}) + a_8\delta(S_{1z}^2 - S_{2z}^2) + \dots , \quad (8)$$

where the suffix \perp stands for projection onto the plane perpendicular to $\hat{\mathbf{L}}$ and higher power of the spin variables have been neglected. The spin components are understood in a frame where the orbital angular momentum is along the z-axis and their values are time-dependent, thus inducing a mild time dependence in ω_m . Note that because of the dependence of the ω_{orb} evolution equation on \mathbf{L} , the spin components parallel to the orbital angular momentum enter already at linear level, whereas the dependence on the spin components in the plane of the orbit starts from the

quadratic level. The a_i coefficients may depend on the symmetric mass ratio ν , but it is assumed here that they can be analytically expanded around their value at $\delta \equiv \sqrt{1 - 4\nu} = (m_1 - m_2)/(m_1 + m_2) = 0$, according to

$$a_i(\delta) = a_i + \delta a_i^{(1)} + \delta^2 a_i^{(2)} + \dots \quad (9)$$

Since the set of simulations analyzed in this work do not include the case of unequal masses, it has been possible to fit only the first term in the expansion (9) for all the coefficients. [35]

Given the specifics of the simulations we used (all having $\delta = 0$ and $\mathbf{S}_2 \cdot \hat{\mathbf{L}} = 0$ initially), it has been possible to determine only the coefficients a_0, a_1, a_3, a_4, a_6 . These values have then been tested against a second set of numerical waveforms, consisting of 8 long waveforms (12-15 cycles long), where all the three phases (inspiral, merger and ring-down) play a role. In particular in the long waveform case, even with the initial condition $\mathbf{S}_2 \cdot \hat{\mathbf{L}} = 0$, the dynamical evolution has lead to generic \mathbf{S}_2 at the time of the onset of the phenomenological phase. Thus the determination of the unknown coefficients $a_{2,7,8,\dots}$ will be necessary for an accurate estimation of ω_m . Additional numerical simulations are required to obtain these extra information and thus improve our model.

The result of the comparison between analytical and numerical waveform is the subject of the next section.

III. RESULTS

The analytical waveforms have been calibrated by comparing them with 24 short numerical simulations, with the result qualitatively shown in figs. 1,2 and quantitatively reported in tab. I.

The determination of the ω_m 's giving the best overlap for different spin values allowed to evaluate some of the coefficients in the phenomenological formula (8), as given in tab. II.

The coefficients $a_{2,5,7,8}$ cannot be determined by the analysis performed because the terms they multiply vanish identically for the 24 simulations considered. The a_0 coefficient has been determined by comparison with a non-spinning waveform[36].

Having fixed the value of ω_m with some generality, it is possible to generate analytical waveforms with any specific initial condition without tuning any single parameter: the value of ω_m will be determined analytically via eq. (8) with the unknown coefficients arbitrarily set to zero. It is then possible to generate waveforms with no tunable parameters for comparison with the second set of long, numerically generated waveforms, even though a wider range of initial conditions would be needed for a more accurate determination of ω_m in the most generic case. Such comparison is summarized qualitatively in fig. 3 and quantitatively in tab. III.

IV. CONCLUSIONS

We presented an analytical method to produce complete gravitational waveforms from spinning coalescing binaries. The free parameters of the model are the values of the orbital frequency at the transition from the inspiral to the phenomenological phase and from the phenomenological to the ring-down phase. They have undergone a calibration process by confronting the analytical waveforms with numerically generated ones and in particular the accurate determination of the first of such parameters (ω_m) turned to be crucial for a satisfactory waveform construction.

For the calibration process a first set of (short) waveforms has been employed, obtaining overlap factors ranging between 0.97 and 0.99. Once the calibration has been obtained, the analytical waveforms, with no parameter to tune, had been confronted with a second set of (long) numerical waveforms and overlap factors ranging from 0.95 to 0.99 have been obtained. Better overlap is expected once a larger number of available numerical waveforms makes it possible to have a more solid estimation of the matching frequency ω_m for generic spins.

The method illustrated here can be extended to produce other modes than the $l = 2, m = 2$ for which it has been tested. The $m = \pm 2$ quadrupolar modes are the only non-vanishing modes for head-on observation of a coalescing system, whereas to build physical waveforms for generic angle between the source and the observer all other modes are required, at least with $l \leq 6$. In particular, as the quality of the numerical waveforms describing such modes improves, it would be interesting to verify if the calibration performed here on the dominant quadrupolar mode allow a good description of other modes.

The programs generating these phenomenological waveforms are written in the C language and are available from the LIGO Analysis Library (LAL) [33].

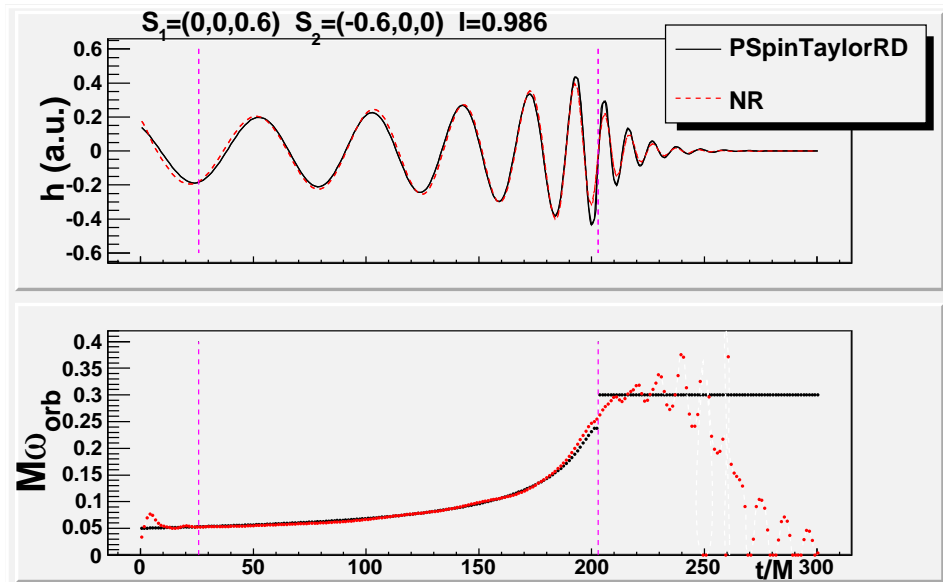


Figure 1: Comparison between the $l = 2, m = 2$ mode of analytical (black, solid) and numerical (red, dashed) equal mass simulations: time-domain waveforms are shown in the upper frame, the lower frame shows ω_{orb} (given respectively by its PN value, by eq.(4) and by ω_{rd} in the three different phases) vs. the instantaneous frequency of the numerical waveform (computed as $\text{Im}(\dot{h}_+ + i\dot{h}_\times)/|h_+ + ih_\times|$, being h_+ (h_\times) the plus (cross) polarization of the numerical waveform). Initial spin configuration: $\mathbf{S}_1/m_1^2 = (0, 0, 0.6)$, $\mathbf{S}_2/m_2^2 = (-0.6, 0, 0)$. Vertical dashed lines mark the onset of the phenomenological phase parametrized by eq. (4) and the ring down phase parametrized by eq. (6). The resulting overlap integral is 0.986.

$\text{acos}(S_1 \hat{L}) [^\circ]$	Overlap	$M\omega_m \times 10^2$	$M\omega_{rd} \times 10^2$
0	0.986	5.29	30.0
15	0.991	5.37	29.5
30	0.991	5.44	28.8
45	0.986	5.49	29.0
60	0.977	5.55	28.0
75	0.975	5.58	28.0
90	0.983	6.07	26.9
105	0.980	6.13	26.5
120	0.981	6.18	26.1
135	0.987	6.00	24.7
150	0.983	6.36	26.4
165	0.984	6.59	26.0
180	0.985	6.47	26.3
195	0.980	6.70	27.0
210	0.980	6.34	27.5
225	0.979	6.29	27.5
240	0.978	6.08	29.9
255	0.977	6.03	28.9
270	0.971	5.68	29.4
285	0.977	5.62	29.6
300	0.980	5.48	30.4
315	0.985	5.51	30.3
330	0.988	5.44	30.3
345	0.988	5.36	29.8

Table I: Values of the overlap integral between the analytical and the 24 short numerical waveforms. For reference, the values of ω_m maximizing the overlap and of ω_{rd} are reported.

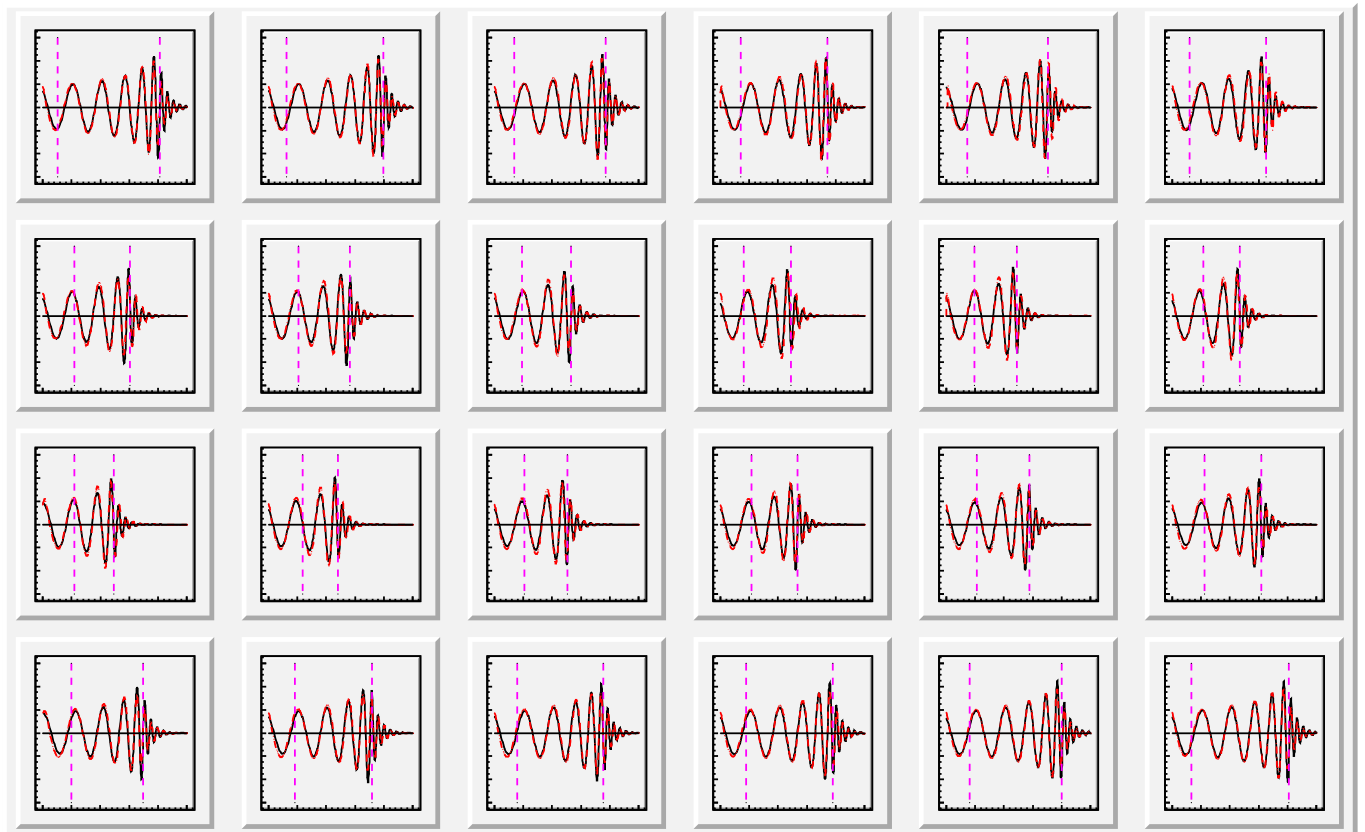


Figure 2: Summary of the comparison between the $l = 2, m = 2$ mode of analytical (black, solid) and numerical (red, dashed) waveforms. Initial spin configuration: $\mathbf{S}_2/m_2^2 = (-0.6, 0, 0)$, \mathbf{S}_1 lies in the x-z plane. A rotation of \mathbf{S}_1 by 15 degrees in the x-z plane takes from one plot to the following one, the first plot is the same as in fig. 1. Vertical dashed lines, x- and y-axis are the same as in fig. 1.

Coeff.	$\times 10^{-2}$
a_0	5.480
a_1	-0.97
a_3	0.083
a_4	0.47
a_6	0.80

Table II: Coefficients of eq.(8) as determined by comparison of the analytical waveforms with 24 short numerical waveforms.

Acknowledgments

It is a pleasure to thank the organizers of the GWDAA-14 conference in Rome for the stimulating scientific environment created by the meeting, as well as Evan Ochsner for useful comments on the paper. R.S. wishes to thank the Physics Department of the University of Massachusetts at Amherst for kind hospitality during the preparation of part of this work. S.F. and L.C. wishes to thank the Università di Urbino for kind hospitality and the Istituto

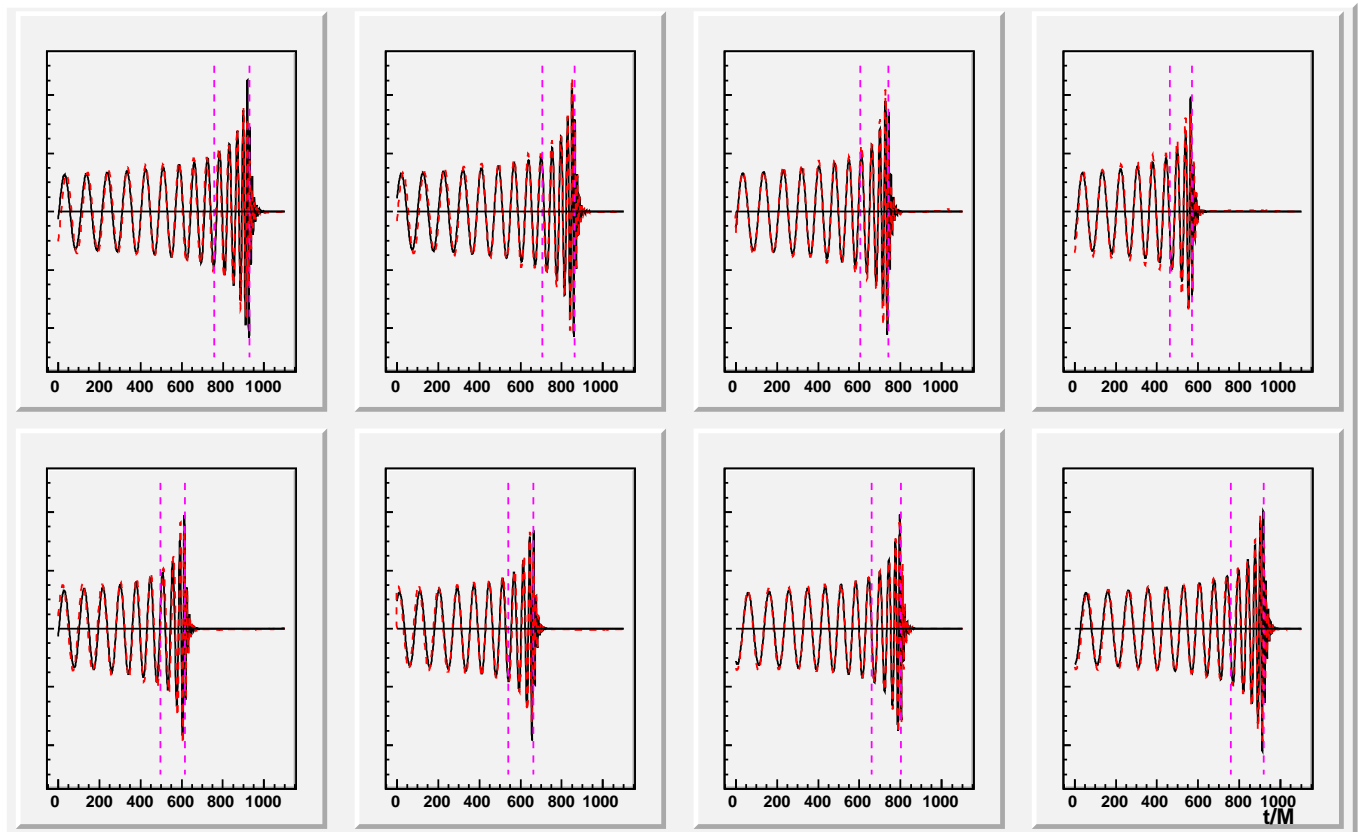


Figure 3: Comparison between the $l = 2, m = 2$ mode of analytical and long numerical waveforms ($m_1 = m_2$). Initial spin configuration: $\mathbf{S}_2/m_2^2 = (-0.6, 0, 0)$, \mathbf{S}_1 lies in the x-z plane. A rotation of \mathbf{S}_1 by 45 degrees in the x-z plane moves the initial condition of one plot to the following one, the first plot refers to the initial condition $\mathbf{S}_1/m_1^2 = (0, 0, 0.6)$. Vertical dashed lines mark the onset of the phenomenological phase and the ring-down phase, x-axis is time in units of M.

$\text{acos}(S_1 \hat{L}) [^\circ]$	Overlap	$M\omega_m \times 10^2$	$M\omega_{rd} \times 10^2$
0	0.9508	5.14	29.2
45	0.9761	5.30	28.6
90	0.9935	5.50	27.2
135	0.9882	5.72	24.9
180	0.9499	5.71	25.4
225	0.9605	5.70	25.9
270	0.9934	5.39	26.7
315	0.9698	5.23	28.3

Table III: Values of the overlap integral between the analytical and the 8 long numerical waveforms. For comparison with the “short” case the values of ω_m and ω_{rd} are reported.

Nazionale di Fisica Nucleare (INFN) for support during the early stage of this work. This work was supported by the INFN and by the NSF grants PHY-0653550, PHY-0925345, PHY-0941417 and PHY-0903973.

References

-
- [1] L. Blanchet, Living Rev. Rel. **9** (2006) 4.
- [2] S. A. Teukolsky, Astrophys. J. **185** (1973) 635.
- [3] F. Pretorius, Phys. Rev. Lett. **95** (2005) 121101 [arXiv: gr-qc/0507014].
- [4] M. Campanelli, C.O. Lousto, P. Marronetti, and Y. Zlochower, Phys. Rev. Lett. **96** (2006) 111101 [arXiv:gr-qc/0511048].
- [5] J.G. Baker, J. Centrella, D. Choi, M. Koppitz and J. van Meter, Phys. Rev. Lett. **96** (2006) 111102 [arXiv:gr-qc/0511103].
- [6] F. Herrmann, I. Hinder, D.M. Shoemaker, P. Laguna and R.A. Matzner, Phys. Rev. D **76** (2007) 084032 [[arXiv:0706.2541]].
- [7] W. Tichy and P. Marronetti, Phys. Rev. D **78** (2008) 081501 [arXiv:0807.2985 [gr-qc]].
- [8] M.A. Scheel, M. Boyle, T. Chu, L.E. Kidder, K.D. Matthews, H.P. Pfeiffer Phys. Rev. D **79** (2009) 024003 [arXiv:0810.1767 [gr-qc]].
- [9] J. G. Baker, W. D. Boggs, J. Centrella, B. J. Kelly, S.T. McWilliams and J.R. van Meter, Phys. Rev. D **78** (2008) 044046 [arXiv:0805.1428 [gr-qc]].
- [10] P. Ajith *et al.*, arXiv:0909.2867 [gr-qc].
- [11] C.O. Lousto, H. Nakano, Y. Zlochower and M. Campanelli, Phys. Rev. D **81** (2010) 084023 [arXiv:0910.3197 [gr-qc]].
- [12] D. Pollney *et al.*, Phys. Rev. D **76** (2007) 124002 [arXiv:0707.2559 [gr-qc]].
- [13] M. Hannam, Class. Quant. Grav. **26** (2009) 114001 [arXiv:0901.2931 [gr-qc]].
- [14] S. Husa, Eur. Phys. J. ST **152** (2007) 183–207.
- [15] F. Pretorius, “Physics of Relativistic Objects in Compact Binaries: From Birth to Coalescence”, Springer, Heidelberg (Germany), 2009 [arXiv:0710.1338].
- [16] LIGO Scientific Collaboration and Virgo Collaboration, “Search for gravitational-wave inspiral signals associated with short Gamma-Ray Bursts during LIGO’s fifth and Virgo’s first science run”, arXiv:1001.0165.
- [17] A. Buonanno and T. Damour, Phys. Rev. D **59** (1999) 084006 [arXiv:gr-qc/9811091].
- [18] A. Buonanno, G. B. Cook and F. Pretorius, Phys. Rev. D **75** (2007) 124018 [arXiv:gr-qc/0610122].
- [19] T. Damour and A. Nagar, Phys. Rev. D **79** (2009) 081503 [arXiv:0902.0136 [gr-qc]].
- [20] Y. Pan, A. Buonanno, L. T. Buchman, T. Chu, L. E. Kidder, H. P. Pfeiffer and M. A. Scheel, arXiv:0912.3466 [gr-qc].
- [21] P. Ajith *et al.*, Class. Quant. Grav. **24** (2007) S689 [arXiv:0704.3764 [gr-qc]].
- [22] A. Buonanno, B. Iyer, E. Ochsner, Y. Pan and B. S. Sathyaprakash, Phys. Rev. D **80** (2009) 084043 [arXiv:0907.0700 [gr-qc]].
- [23] E. Racine, A. Buonanno and L. E. Kidder, Phys. Rev. D **80** (2009) 044010 [arXiv:0812.4413 [gr-qc]].
- [24] K. G. Arun, A. Buonanno, G. Faye and E. Ochsner, Phys. Rev. D **79** (2009) 104023 [arXiv:0810.5336 [gr-qc]].
- [25] J. G. Baker, J. R. van Meter, S. T. McWilliams, J. Centrella and B. J. Kelly, Phys. Rev. Lett. **99** (2007) 181101 [arXiv:gr-qc/0612024].
- [26] M. Boyle *et al.*, Phys. Rev. D **76** (2007) 124038 [arXiv:0710.0158 [gr-qc]].
- [27] A. Buonanno, Y. Pan, J. G. Baker, J. Centrella, B. J. Kelly, S. T. McWilliams and J. R. van Meter, Phys. Rev. D **76** (2007) 104049 [arXiv:0706.3732 [gr-qc]].
- [28] E. Berti, V. Cardoso and C. M. Will, Phys. Rev. D **73** (2006) 064030 [arXiv:gr-qc/0512160].
- [29] E. Barausse and L. Rezzolla, Astrophys. J. **704** (2009) L40 [arXiv:0904.2577 [gr-qc]].
- [30] E. Schnetter, S.H. Hawley and I. Hawke, Class. Quant. Grav (2004) **21** 1465–1488 [arXiv:0310042 [gr-qc]].
- [31] Cactus Computational Toolkit home page: <http://www.cactuscode.org>.
- [32] S. Husa, I. Hinder and C. Lechner, Computer Physics Communications **174** (2006) 983-1004 [arXiv:0404023 [gr-qc]].
- [33] <https://www.lsc-group.phys.uwm.edu/daswg/projects/lal.html>
- [34] Clearly the approximation of constant ι and α in the phenomenological phase is a brutal one and it can be badly wrong in the case of strongly precessing systems (like systems with $\nu \ll 1$ where the more massive body has (nearly-)extremal spin not-aligned with the orbital angular momentum. However in those cases a phenomenological formula in the same spirit of eq. (4) can be written for ι and α .
- [35] Note that from the explicit formula for ω_{orb} , see e.g. [22], symmetric combinations of the spin components can only depend analytically on the symmetric mass ratio ν , and thus will depend on even power of δ , whereas anti-symmetric combinations do not appear for $\delta = 0$.
- [36] Note that given the moderate value of the spin magnitude, the plane of the orbit relative to these waveforms are only “mildly” precessing.